

# Jerk, Speed, and Acceleration on Inclined Surfaces

Mateo Patino<sup>a)</sup> and Clinton Nash<sup>b)</sup>

*Thornton Academy, 438 Main Street, Saco, Maine 04072, USA*

<sup>a)</sup>mateo.patino25@thorntonacademy.org

<sup>b)</sup>Corresponding author: clinton.nash@thorntonacademy.org

**Abstract.** An algorithm is developed to generate the equations defining vertical plane curves such that objects placed on them experience constant kinematic jerk. Two different types of constant jerk are explored. The first is simply the tangential component of the total jerk, and the second is the time rate of change of the magnitude of the tangential component of acceleration. The latter corresponds most directly to the notion of changes in the rate of change of speed. The curves so developed were calculated numerically and are almost parabolic.

## INTRODUCTION

What sort of surface curvature results in a constant tangential jerk for a sliding object? This is the question we address in this paper. Its answer is not obvious and, as far as we can tell, it is not to be found explicitly within the canon of elementary mechanics [1]. If present at all, discussions of jerk in physics textbooks rarely venture much beyond its amusing name [2]. This is perhaps surprising since, as the time derivative of acceleration, jerk represents a straightforward extension of standard kinematics [3].

In this contribution, we first seek the vertical plane curve  $y(x)$  upon which a sliding object has a tangential jerk of constant magnitude,  $j_T$ . Second, we seek a different vertical plane curve defined by the property that a sliding object experiences a tangential acceleration whose magnitude changes linearly with time; that is,  $\dot{a}_T$  is constant. It is tempting to imagine that these two curves are identical owing to the relationship between jerk and acceleration, but the following analysis reveals that they are not. Assuming  $\alpha$  represents the local angle of  $y(x)$  according to Fig. 1, the total jerk  $\vec{j} = \frac{d}{dt}(a_T\hat{T} + a_N\hat{N})$  can be simplified via the identities  $\hat{T} = \pm\alpha\hat{N}$  and  $\hat{N} = \pm\alpha\hat{T}$  to show that the tangential jerk  $j_T$  is a function of  $\dot{a}_T$ :  $\vec{j} = \dot{a}_T\hat{T} + a_T\dot{\hat{T}} + \dot{a}_N\hat{N} + a_N\dot{\hat{N}} = (\dot{a}_T \pm a_N\dot{\alpha})\hat{T} + (\dot{a}_N \pm a_T\dot{\alpha})\hat{N}$ .

This demonstrates that  $j_T = \dot{a}_T \pm a_N\dot{\alpha}$ , so a curve where the quantity  $\dot{a}_T$  is constant must differ from one where  $j_T$  is constant. Our purpose in this work is to derive  $\dot{a}_T$  and  $j_T$ , generate  $y(x)$  numerically from each expression, and further distinguish each curve by exploring their geometric characteristics.

## THEORY

### Tangential Component of Jerk

We consider an object of constant mass  $m$  subject to gravity and a normal force that slides without friction down an inclined surface,  $y(x)$ , having a variable slope (Fig. 1). According to Newton's second law, the vector sum of these forces is proportional to the instantaneous acceleration of the object,  $\vec{a} = \frac{\vec{F}_{\text{net}}}{m} = \frac{1}{m}(\vec{F}_N + m\vec{g}) = \frac{\vec{F}_N}{m} + \vec{g}$ .

The normal force  $\vec{F}_N$  can be expressed as  $\vec{F}_N = \left(mg \cos \alpha + \frac{mv^2}{R}\right)\hat{N}$ .

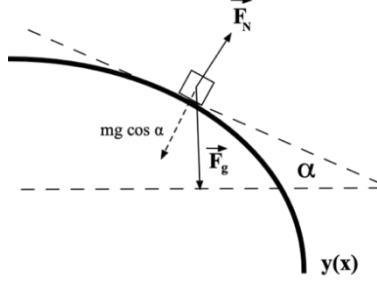


**FIGURE 1.** Vertical plane curve  $y(x)$  characterized by a variable tangential acceleration.  $\alpha$  denotes the local angle of the curve and can be related to the geometry of  $y(x)$  via  $\sin \alpha = \frac{-y'(x)}{\sqrt{1+y'(x)^2}}$

By definition, jerk is the time derivative of  $\vec{a}$ , which gives

$$\vec{j} = \frac{d\vec{a}}{dt} = \frac{d}{dt} \left( \frac{1}{m} \left( mg \cos \alpha + \frac{mv^2}{R} \right) \hat{N} + \vec{g} \right) = \frac{d}{dt} \left( \left( g \cos \alpha + \frac{v^2}{R} \right) \hat{N} \right), \quad (1)$$

where  $g \cos \alpha$  is the normal component of the gravitational acceleration and  $v^2/R$  is a speed-dependent centripetal acceleration that involves the signed osculating radius  $R$ .  $\vec{j}$  can be found by rewriting these quantities and the unit vectors  $\hat{T}$  and  $\hat{N}$  in terms of  $y(x)$  and its higher-order derivatives, a process available in Appendix A. There we demonstrate that jerk resolves into tangential and normal components,  $\vec{j} = j_T \hat{T} + j_N \hat{N}$ . These components have magnitudes

$$j_T = \frac{-gy''(x)v}{(1+y'(x)^2)^2} - f \frac{y''(x)^2 v^3}{(1+y'(x)^2)^3} \quad (2)$$

and

$$j_N = \frac{fv^3 \sqrt{y'''(x)^2}}{(1+y'(x)^2)^2} \left( \frac{-2gy'(x)}{v^2} + \frac{y'''(x) + y'''(x)y'(x)^2 - 3y'(x)y''(x)^2}{y''(x)(1+y'(x)^2)} \right) - \frac{gy'(x)y''(x)v}{(1+y'(x)^2)^2}, \quad (3)$$

where the factor  $f = \pm 1$  is introduced to account for the sign of the osculating radius according to the conventions in Appendix B. The derivation of the normal component jerk is highly involved, as it includes the derivative of an absolute value function and a third derivative of  $y(x)$ . For the sake of simplicity and because it is not our primary focus, we simply report the result here.

## Time-Dependent Tangential Acceleration

In contrast to Eqs. (2) and (3), the derivation of  $\dot{a}_T$  is straightforward and starts with the well-known expression for the tangential acceleration on an inclined surface,

$$a_T = g \sin \alpha = \frac{d^2 s}{dt^2} = \frac{-gy'(x)}{\sqrt{1+y'(x)^2}}. \quad (4)$$

By taking advantage of the relationship between  $\alpha$  and the geometry of  $y(x)$  and using implicit differentiation,  $\dot{a}_T$  can be calculated as the time derivative of Eq. (4),

$$\dot{a}_T = \frac{da_T}{dt} = \frac{d^3 s}{dt^3} = \frac{-gy''(x)v}{(1+y'(x)^2)^2}. \quad (5)$$

As noted earlier,  $\dot{a}_T$  and  $j_T$  are related to each other in a nontrivial way. This relationship is explained in detail in terms of  $y(x)$  and physical quantities in Appendix C.

## Numerical Solutions

The surfaces we seek are  $y(x)$  solutions to Eq. (2) for a constant value of  $j_T$  or solutions to Eq. (5) for a constant value of  $\dot{a}_T$ . It seems highly unlikely that analytical solutions exist, but both equations are well suited to be solved with numerical methods. In particular, Eq. (2) can be rearranged to a convenient quadratic form with respect to  $y''(x)$ , which provides an expression for  $y''(x)$  through the quadratic formula. After simplification, we have

$$y''(x) = \frac{1+y'(x)^2}{2fv^2} \left( -g + \sqrt{g^2 - 4fv(1+y'(x)^2)j_T} \right). \quad (6)$$

At the same time, the  $\dot{a}_T$  equation, Eq. (5), can be rearranged to give

$$y''(x) = \frac{-\dot{a}_T}{gv} (1+y'(x)^2)^2. \quad (7)$$

Because of the  $y$  dependence of speed under conservation of energy, speed can be expressed as  $v = \sqrt{v_0^2 + 2g(y_0 - y(x))}$  and Eqs. (6) and (7) can each be recast as a set of coupled, autonomous differential equations  $u(x) = y'(x)$  and  $u'(x) = y''(x)$ , which we have solved by implementing a fourth-order Runge-Kutta algorithm. In both cases, these systems of equations are autonomous, meaning that their solution requires no explicit reference to time. We implemented the RK4 solution to these systems in an open-source software package named Jcurve, which also offers more tools to explore and analyze the resulting surfaces [4].

## RESULTS AND DISCUSSION

We have applied Jcurve to two cases of constant  $j_T$  and constant  $\dot{a}_T$ . Case A represents a curve with a positive  $j_T$  and  $\dot{a}_T$  and the initial conditions  $\dot{a}_T, j_T = 2 \text{ m/s}^3$ ,  $a_0 = 0$ , and  $v_0 = 1 \text{ m/s}$ . Case B exemplifies a curve with a negative  $j_T$  and  $\dot{a}_T$  and the initial conditions  $\dot{a}_T, j_T = -4 \text{ m/s}^3$ ,  $a_0 = 7 \text{ m/s}^2$ , and  $v_0 = 0.001 \text{ m/s}$  (this speed was chosen instead of  $v_0 = 0$  to avoid numerical instability). The resulting curves are displayed in Fig. 2.

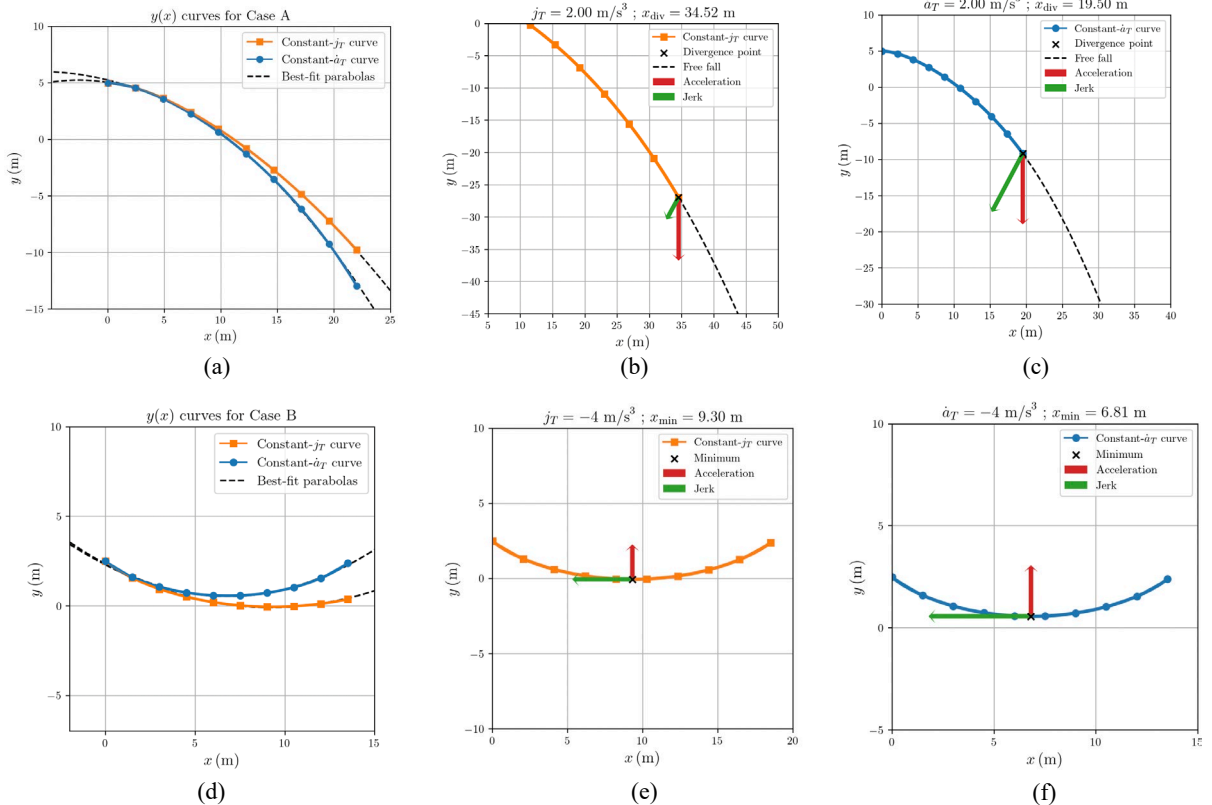


**FIGURE 2.**  $y(x)$  surfaces from cases A and B. (a) Curves with a constant  $\dot{a}_T$  and  $j_T$  of  $2 \text{ m/s}^3$  (only 22 m of the curves' horizontal length are displayed, but they extend further). These surfaces are concave-down and nearly parabolical, as the best-fit parabolas match the numerically calculated curves with an  $R^2$  score of  $R^2 = 0.99985$  for the  $j_T$  curve and  $R^2 = 0.99983$  for the  $\dot{a}_T$  curve. (b) Critical behavior of case A  $j_T$  surface. As the object slides down the curve, there is a point where the gravitational acceleration is insufficient to keep the object in contact with the surface; we refer to this location as the divergence point  $x_{\text{div}}$ . For the  $j_T$  curve, the object diverges from  $y(x)$  at  $x_{\text{div}} = 34.52 \text{ m}$  at a speed  $v = 25.04 \text{ m/s}$ . (c) Critical behavior of case A  $\dot{a}_T$  surface. This surface has a divergence point  $x_{\text{div}} = 19.50 \text{ m}$  where the object enters free fall at  $v = 16.70 \text{ m/s}$ . (d) Curves with a constant  $\dot{a}_T$  and  $j_T$  of  $-4 \text{ m/s}^3$  (only 13.5 m of the curves' horizontal length are shown). These surfaces are concave-up and can be approximated with a parabola, achieving  $R^2 = 0.99623$  for the  $j_T$  curve and  $R^2 = 0.99601$  for the  $\dot{a}_T$  curve. (e) Critical behavior of case B  $j_T$  curve. Surfaces with negative jerk have a critical minimum instead of a divergence point; for this curve,  $x_{\text{min}} = 9.30 \text{ m}$ . (f) Critical behavior of case B  $\dot{a}_T$  curve. This surface reaches its critical minimum at  $x_{\text{min}} = 6.81 \text{ m}$ .

Figure 2 shows interesting features of the  $y(x)$  surfaces we sought. On one hand, curves with a positive  $j_T$  or  $\dot{a}_T$  possess a divergence point after which the sliding object enters free fall. In case A, the divergence point of the constant- $j_T$  curve is 77% further away from the start of the trajectory than that of the constant  $\dot{a}_T$  curve. This large difference in divergence values belies how close the curves track each other for the first 10 m or so, as shown in Fig. 2(a). Only when the curve becomes steep and the normal component of acceleration changes quickly do they differ significantly. On the other hand, curves with a negative  $j_T$  or  $\dot{a}_T$  do not have divergence points, but they bottom out and reverse direction. In case B, the location of the critical minima is affected by the horizontal length of each curve. Owing to the high initial acceleration and the corresponding rapid change in the magnitude of normal acceleration in case B, the  $j_T$  and  $\dot{a}_T$  curves diverge almost immediately, so they reach different horizontal extensions and drag the minimum point accordingly.

In both cases A and B, surfaces generated with constant  $j_T$  do not bend as much as those with the same value of constant  $\dot{a}_T$ ; they do not need to. For the former, the tangential jerk caused by the curvature is augmented by the tangential component of the derivative of the acceleration perpendicular to the curve. We encourage the reader to examine Appendix D, where the components of jerk for each surface are displayed and this relationship is better depicted. The plots in this appendix also shine a light on a characteristic of tangential and scalar jerk that may not come as a surprise: surfaces defined by constant  $j_T$  are marked by varying  $\dot{a}_T$  and vice versa.

The surfaces in both cases A and B, as well as every other curve we tested, are nearly parabolic. Almost an exact agreement can be reached between the numerical curve and polynomials as high as fifth order in all the cases we studied, but of course, that does not mean anything about the nature of constant-jerk curves except that they are well behaved. Slightly better agreement is achieved when the curves are fit to a flattened catenary; again, however, this agreement is imperfect. One might hope for an analytical curve that confers this type of motion, similar to how the cycloid corresponds to brachistochrone curves, but our results suggest no such surface exists.

## CONCLUSION

Our question has been answered: inclined surfaces producing constant tangential jerk are curved in a way that is almost parabolic. There may be no simple explanation for this except to follow the mathematics, which is not particularly satisfying. A natural follow-up question might concern how the shape of a constant-tangential-jerk surface is different if an object rolls without slipping rather than sliding down it. In fact, it is straightforward to move beyond a frictionless scenario to incorporate rolling into this kind of analysis.

## ACKNOWLEDGMENTS

We want to thank Matthew Amoroso and Brian Laich for their helpful comments about this work. We would also like to thank the reviewer for extremely insightful suggestions which have greatly enhanced the clarity of our contribution.

## REFERENCES

1. H. Hayati, D. Eager, A.-M. Pendrill, and H. Alberg, *Vib.* **3**, 371–409 (2020).
2. T. R. Sandlin, *Phys. Teach.* **28**, 36–40 (1990).
3. S. Schot, *Am. J. Phys.* **46**, 1090–1094 (2023).
4. M. Patino and C. Nash, *Jcurve* [computer software]. Available at <https://github.com/mateo-patino/jcurve>.

## APPENDIX A

Starting with the definition of jerk established in Eq. (1), we make use of the identities  $\sin \alpha = \frac{-y'(x)}{\sqrt{1+y'(x)^2}}$  and  $\cos \alpha = \frac{1}{\sqrt{1+y'(x)^2}}$ , to get

$$\vec{j} = \frac{d\vec{a}}{dt} = \frac{d}{dt} \left( \left( g \cos \alpha + \frac{v^2}{R} \right) \hat{N} \right) = \hat{N} \frac{d}{dt} \left( \frac{g}{\sqrt{1+y'(x)^2}} + \frac{v^2}{R} \right) + \left( \frac{g}{\sqrt{1+y'(x)^2}} + \frac{v^2}{R} \right) \frac{d\hat{N}}{dt}. \quad (8)$$

In this representation, the normal and tangential unit vectors are

$$\hat{N} = \frac{-y'(x)\hat{i} + \hat{j}}{\sqrt{1+y'(x)^2}} \quad \text{and} \quad \hat{T} = \frac{\hat{i} + y'(x)\hat{j}}{\sqrt{1+y'(x)^2}}$$

Making use of the implicit differentiation of  $y(x)$ ,

$$\frac{dy(x)}{dt} = \frac{dy}{dx} \frac{dx}{dt} = \frac{dy}{dx} v_x = \frac{y'(x)v}{\sqrt{1+y'(x)^2}},$$

it can easily be seen that

$$\frac{d\hat{N}}{dt} = \frac{d}{dt} \left( \frac{-y'(x)}{\sqrt{1+y'(x)^2}} \right) \hat{i} + \frac{d}{dt} \left( \frac{1}{\sqrt{1+y'(x)^2}} \right) \hat{j} = \frac{y''(x)v}{(1+y'(x)^2)^{\frac{3}{2}}} (-\hat{T}).$$

Therefore, Eq. (8) resolves into components  $\vec{j} = j_T \hat{T} + j_N \hat{N}$ , where

$$j_T = - \left( \frac{g}{\sqrt{1+y'(x)^2}} + \frac{v^2}{R} \right) \frac{y''(x)v}{(1+y'(x)^2)^{\frac{3}{2}}} \quad (9)$$

and

$$j_N = \frac{d}{dt} \left( \frac{g}{\sqrt{1+y'(x)^2}} + \frac{v^2}{R} \right). \quad (10)$$

To simplify Eqs. (9) and (10), it is necessary to introduce the explicit formula for the reciprocal of the osculating radius  $R$ ,

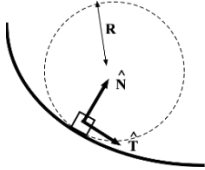
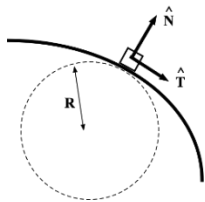
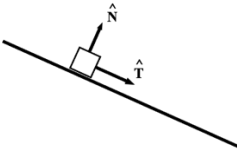
$$\frac{1}{R} = \frac{f}{|v|} \left| \frac{d\hat{T}}{dt} \right| = f \left| \frac{y''(x)}{(1+y'(x)^2)^{\frac{3}{2}}} \right|, \quad (11)$$

where factor  $f = \pm 1$  is related to the sign of  $R$ . Substituting this equation into Eq. (9), we obtain the expression for the magnitude of the tangential component of jerk,

$$j_T = \frac{-gy''(x)v}{(1+y'(x)^2)^2} - \frac{1}{R} \left( \frac{y''(x)v^3}{(1+y'(x)^2)^{\frac{3}{2}}} \right) = \frac{-gy''(x)v}{(1+y'(x)^2)^2} - f \frac{y''(x)^2 v^3}{(1+y'(x)^2)^3}.$$

## APPENDIX B

**TABLE 1.** Conventions relating the sign of the osculating radius  $R$  to the value of  $f$ .

$R$	$f$	Related Quantities	Scenario
$R > 0$	1	$y''(x) > 0$ $j_T < 0$	
$R < 0$	-1	$y''(x) < 0$ $j_T > 0$	
$R \rightarrow \infty$	1	$y''(x) = 0$ $j_T = 0$	

## APPENDIX C

The expression for  $\dot{a}_T$ ,

$$\dot{a}_T = \frac{da_T}{dt} = \frac{d^3s}{dt^3} = \frac{-gy''(x)v}{(1+y'(x)^2)^{3/2}},$$

is clearly the first term in the expression for  $j_T$ , Eq. (2), a fact that lays bare the close relationship between constant- $j_T$  curves and constant- $\dot{a}_T$  curves while demonstrating conclusively that they are not the same. It can be proved that the second term in Eq. (2), which accounts for the difference in  $\dot{a}_T$  and  $j_T$ , is the tangential component of the time derivative of the normal (radial) component of acceleration,  $a_N \hat{\mathbf{N}}$ ,

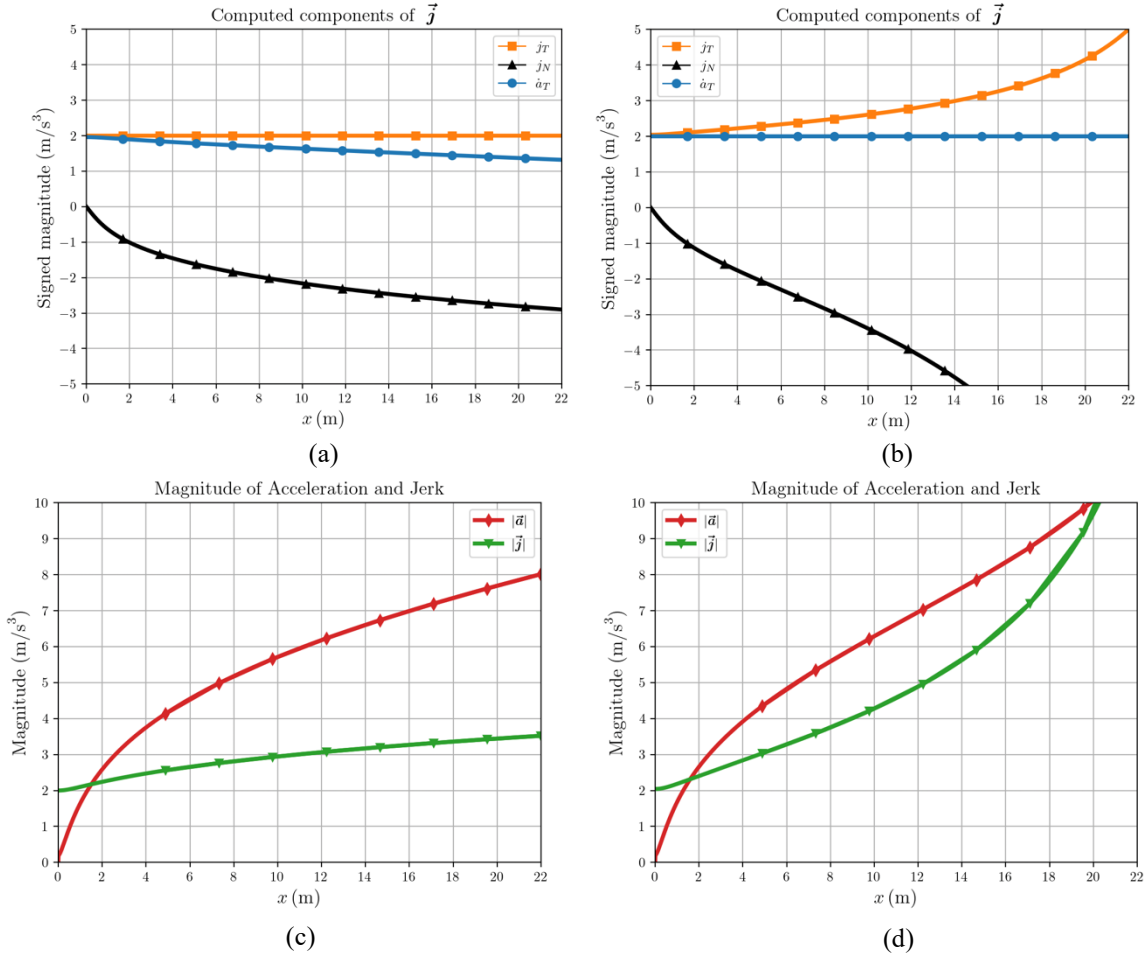
$$\frac{d}{dt}(a_N \hat{\mathbf{N}}) = \frac{da_N}{dt} \hat{\mathbf{N}} + a_N \frac{d\hat{\mathbf{N}}}{dt} = \frac{da_N}{dt} \hat{\mathbf{N}} - a_N \frac{y''(x)v}{(1+y'(x)^2)^{3/2}} \hat{\mathbf{T}}.$$

Using the reciprocal of the osculating radius, Eq. (11), the tangential component becomes

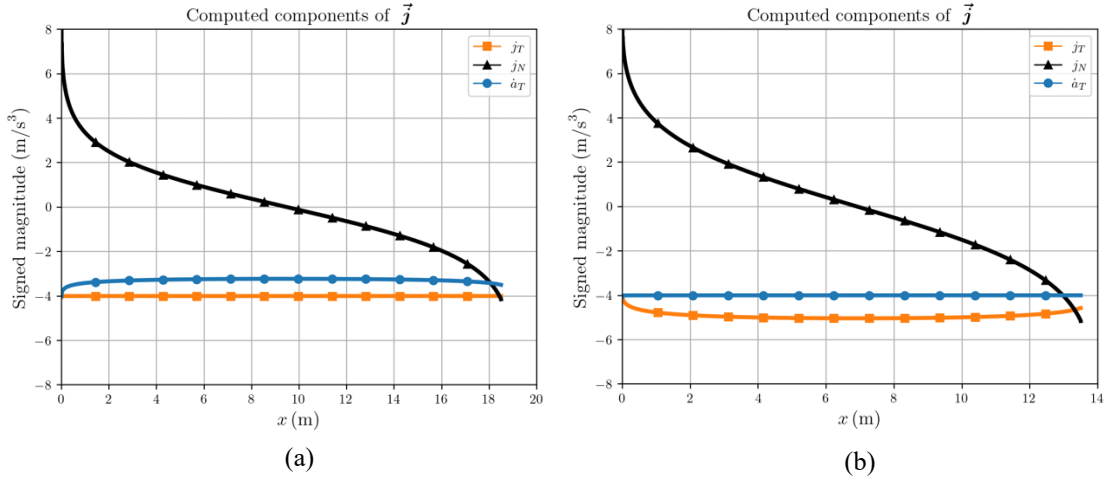
$$\frac{-v^2}{R} \frac{y''(x)v}{(1+y'(x)^2)^{3/2}} \hat{\mathbf{T}} = - \left| \frac{y''(x)}{(1+y'(x)^2)^{3/2}} \right| \frac{y''(x)v^3}{(1+y'(x)^2)^{3/2}} \hat{\mathbf{T}} = -f \frac{y''(x)^2 v^3}{(1+y'(x)^2)^3} \hat{\mathbf{T}},$$

whose magnitude is evidently the second term of  $j_T$ .

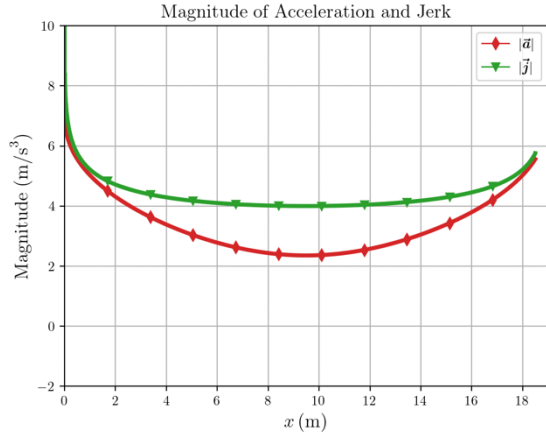
## APPENDIX D



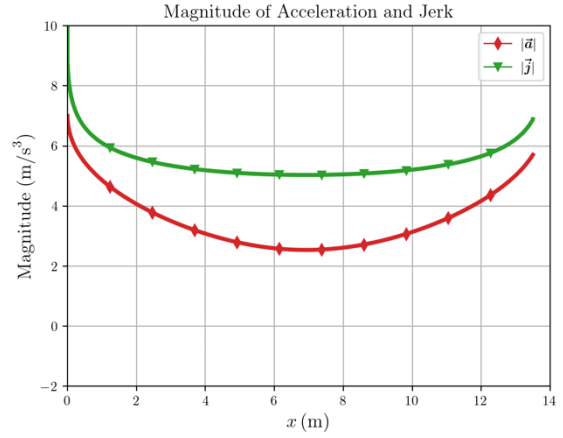
**FIGURE 3.** Dynamical data of case A curves. (a) Magnitudes of  $j_T$ ,  $j_N$ , and  $a_T$  for constant- $j_T$  curve. (b) Magnitudes of  $j_T$ ,  $j_N$ , and  $a_T$  for constant- $a_T$  curve. (c)  $|\vec{a}|$  and  $|\vec{j}|$  for constant- $j_T$  curve. (d)  $|\vec{a}|$  and  $|\vec{j}|$  for constant- $a_T$  curve.







(c)



(d)

**FIGURE 4.** Dynamical data of case B curves. (a) Magnitudes of  $j_T$ ,  $j_N$ , and  $\dot{a}_T$  for constant- $j_T$  curve. (b) Magnitudes of  $j_T$ ,  $j_N$ , and  $\dot{a}_T$  for constant- $\dot{a}_T$  curve. (c)  $|\vec{a}|$  and  $|\vec{j}|$  for constant- $j_T$  curve. (d)  $|\vec{a}|$  and  $|\vec{j}|$  for constant- $\dot{a}_T$  curve.

## APPENDIX E

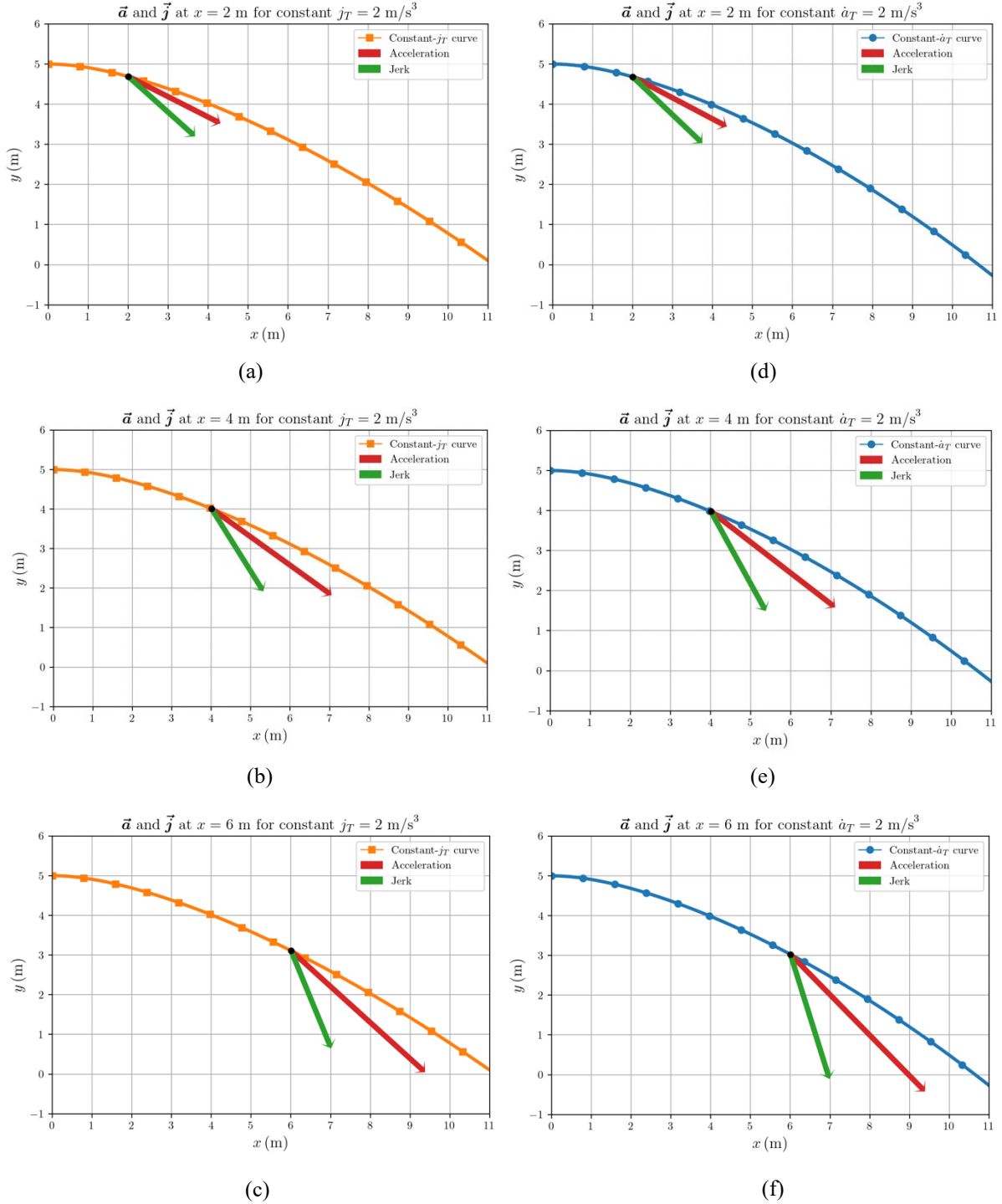
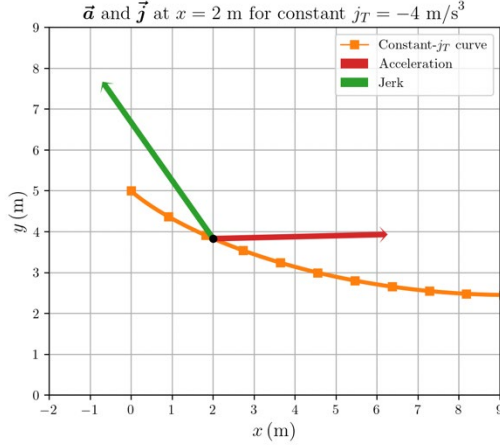
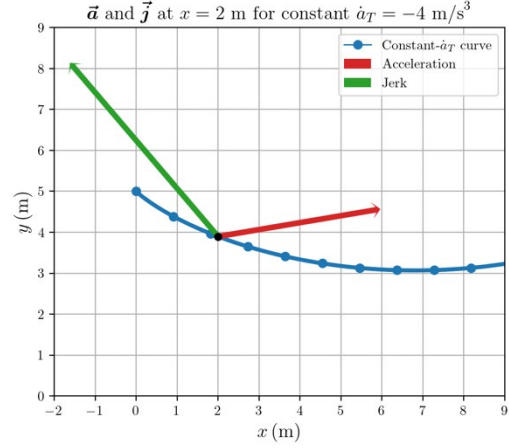


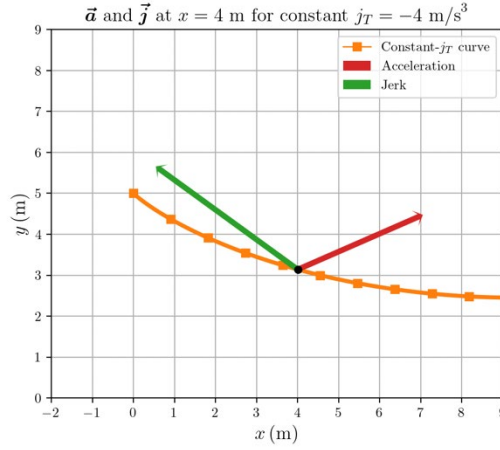
**FIGURE 5.** Evolution of  $\vec{a}$  and  $\vec{j}$  along 10 m of case A curves. (a)  $\vec{a}$  and  $\vec{j}$  at  $x = 2$  m for  $j_T$  curve. (b)  $\vec{a}$  and  $\vec{j}$  at  $x = 4$  m for  $j_T$  curve. (c)  $\vec{a}$  and  $\vec{j}$  at  $x = 6$  m for  $j_T$  curve. (d)  $\vec{a}$  and  $\vec{j}$  at  $x = 2$  m for  $\dot{a}_T$  curve. (e)  $\vec{a}$  and  $\vec{j}$  at  $x = 4$  m for  $\dot{a}_T$  curve. (f)  $\vec{a}$  and  $\vec{j}$  at  $x = 6$  m for  $\dot{a}_T$  curve.



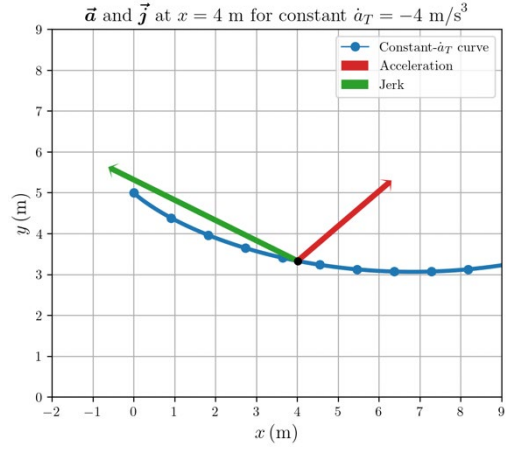
(a)



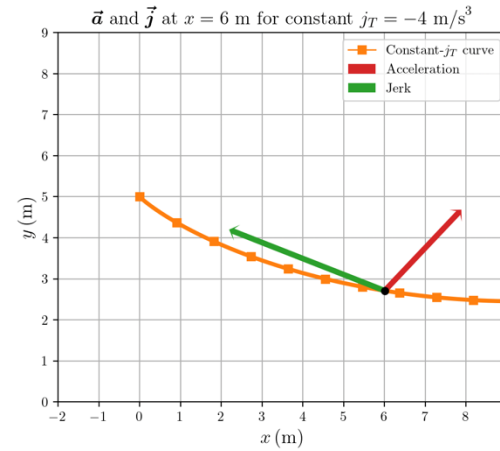
(d)



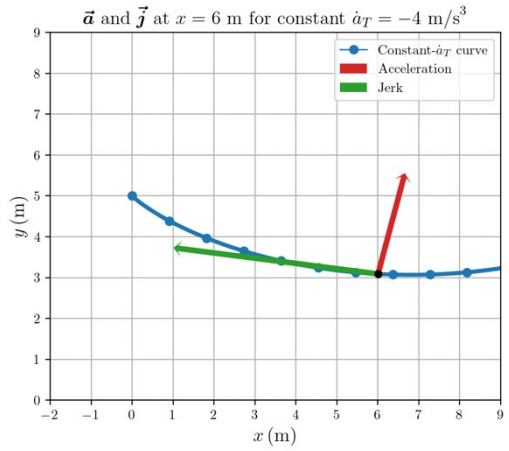
(b)



(e)



(c)



(f)

**FIGURE 6.** Evolution of  $\vec{a}$  and  $\vec{j}$  along 10 m of case B curves. (a)  $\vec{a}$  and  $\vec{j}$  at  $x = 2$  m for  $j_T$  curve. (b)  $\vec{a}$  and  $\vec{j}$  at  $x = 4$  m for  $j_T$  curve. (c)  $\vec{a}$  and  $\vec{j}$  at  $x = 6$  m for  $j_T$  curve. (d)  $\vec{a}$  and  $\vec{j}$  at  $x = 2$  m for  $\dot{a}_T$  curve. (e)  $\vec{a}$  and  $\vec{j}$  at  $x = 4$  m for  $\dot{a}_T$  curve. (f)  $\vec{a}$  and  $\vec{j}$  at  $x = 6$  m for  $\dot{a}_T$  curve.